Polymers **2011**, *3*, 1554-1564; doi:10.3390/polym3031554

OPEN ACCESS

polymers

ISSN 2073-4360

www.mdpi.com/journal/polymers

Article

Polymeric Optical Code-Division Multiple-Access (CDMA) Encoder and Decoder Modules

Xuejun Lu [1,*] and Ray T. Chen [2]

[1] Department of Electrical and Computer Engineering, University of Massachusetts Lowell, 1 University Avenue, Lowell, MA 01854, USA

[2] Microelectronics Center, University of Texas Austin, 10100 Burnet Rd, Austin, TX 78758, USA; E-Mail: raychen@uts.cc.utexas.edu

* Author to whom correspondence should be addressed; E-Mail: xuejun_lu@uml.edu; Tel.: +1-978-934-3359; Fax: +1-978-934-3027.

Received: 1 August 2011; in revised form: 31 August 2011 / Accepted: 13 September 2011 / Published: 19 September 2011

Abstract: We propose a low cost polymeric optical waveguides-based optical CDMA encoder and decoder modules. The structures of the optical CDMA encoder and decoder modules are presented. The performance of the optical CDMA encoder and decoder modules is simulated using 10-chip binary phase-shift keying (BPSK) coding schemes. The optical CDMA encoder and decoder modules can effectively transmit and recover optical CDMA data streams. The SNR of the received signal is analyzed and determined to be primarily from the cross correlation with other channels.

Keywords: polymer optical waveguide; optical CDMA; thermal optical effect

1. Introduction

Code-Division Multiple-Access (CDMA) is a spectrum-spreading technique that enables many users to share transmission bandwidth with individual addressing capabilities through the allocation of specific access codes [1]. The spectrum-spreading multiplexing scheme not only provides much higher bandwidth efficiency for a given spectrum allocation than traditional multiplexing approaches, such as frequency-division multiplexing (FDM) and time-division multiplexing (TDM), but also allows robust

and secure communication over open and time-varying channels [1,2]. Due to these advantages, CDMA technology has been employed extensively in numerous military and civilian applications, such as Radar, remote sensing and cellular phones in the microwave region (300 MHz–300 GHz) [1,2].

The working principle of CDMA technology in optical region (C-band 1,530–1,560 nm, and L-band 1,560–1,611 nm) (optical CDMA) is essentially the same as the CDMA technology in the microwave region (microwave CDMA). In optical CDMA, data-streams from different subscribers are phase or frequency encoded by the pre-defined access codes called chips. The length of the code corresponds to the chip number. Each bit of the original optical CDMA data streams (*i.e.*, a symbol) is coded by the M pre-defined codes, where M is the code length or chip number. The encoded data streams from individual subscribers are combined through a passive Mx1 coupler and then sent to optical networks. The received data streams are split through a 1 × M splitter and finally decoded by the predefined code sequences. Optical CDMA as an alternative to other optical multiplexing schemes such as wave-length division multiplexing (WDM) and TDM, not only inherits the advantages of microwave CDMA such as efficient bandwidth usage, robust and secure communication over open channels, but also has many additional attractive features including higher granularity and scalability within optical networks, optical transparency to data format and rate, improved cross-talk performance and more flexible asynchronous access [3-8]. In addition, optical CDMA scheme avoids the optical-to-electrical and electrical-to-optical conversion processes and eliminates the bandwidth constrains set by conventional electronics technologies (<10 GHz). It offers much higher speed for data transport and routing than electronic counterparts. Due to these advanced features, optical CDMA is a promising technology for next-generation ultra-high speed, cost-effective broadband access network.

Polymeric waveguide based photonics devices have been extensively researched [9-15]. Electro-optic (EO) polymers with high EO coefficients have been developed [14,15]. High performance polymer EO modulators have also been developed [10-13]. Polymers also have a large thermo-optic (TO) coefficient which can be used for the development of optical switches and variable optical attenuators (VOA). In addition, since polymeric waveguides can be fabricated by spin-coating on virtually any devices without any lattice mismatching constrain, they are promising candidates for integrated optical devices and optical interconnect. Compared with optical fibers, polymeric waveguides can be fabricated to the sub-micrometer accuracy by using the state-of-the-art photolithography technologies. This enables one to achieve optical delay lines with femto-second (fs) accuracy. The advantages of polymeric waveguides, including high EO and TO coefficients, compatible with other electronics and optoelectronics, and capability to make ultra-high accuracy time delay lines, make them promising material for photonics devices. In this paper, we propose low cost polymeric waveguide based optical CDMA encoder and decoder modules suitable for FTTH applications. The structures of the optical-CDMA encoder and decoder modules are presented. The working mechanisms are illustrated. The performances are simulated and analyzed.

2. Device Structures and Working Principle

The schematic structure of the proposed optical CDMA encoder for a channel is shown in Figure 1. It consists of ten 10% tap couplers, optical time-delay lines, and phase-encoders. Each of the time-delay lines is designed to provide a 5 picosecond (ps) time-delay. Since the binary phase-shift keying (BPSK) is one of the commonly used coding schemes in conventional CDMA systems, we use the

BPSK coding scheme in the optical CDMA system as well. The time-delayed data streams are phase-encoded by the integrated phase-encoders (BPSK). Each channel has its own BPSK codes. For example, the channel #1 codes are [0 π 0 0 0 π π 0 π 0] and the channel #2 codes are [0 π 0 0 π 0 0 0 0 π]. The BPSK coded data streams are finally combined and sent out through the optical CDMA output waveguide.

Figure 1. Schematic structure of the proposed optical Code-Division Multiple-Access (CDMA) encoder. It consists of ten 10% tap couplers, optical time-delay lines, and phase-encoders. Each of the time-delay lines is designed to provide a 5 ps time-delay. The time-delayed data streams are phase-encoded by the integrated phase-encoders. The phase-encoded data streams are finally combined and sent out through the optical CDMA output waveguide.

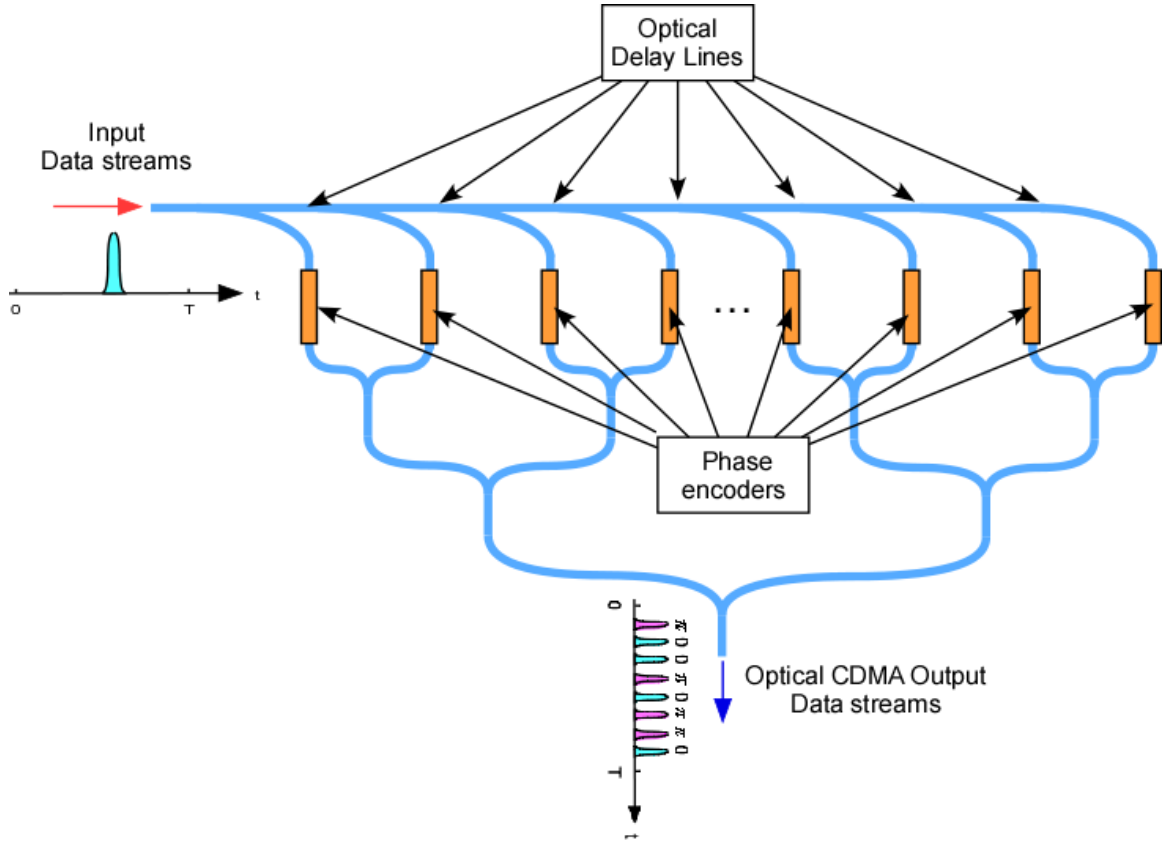

The structure of the polymeric thermo-optic (TO) phase encoder is shown in Figure 2. It consists of a polymeric waveguide with a top electrode. The top electrode and the polymeric waveguide are separated by a cladding layer. Local heating in the polymeric waveguide can be achieved by applying current through the top electrode. The top electrode can thus function as a local heater. The current heater increases the temperature of the polymeric waveguide. The temperature increase will lead to refractive index change through the TO effect of the polymeric waveguide [14]. The thermo-optics efficient ($\partial n/\partial T$) of the polymeric waveguide is typically $\partial n/\partial T \sim -2 \times 10^{-4}$ K^{-1} [14,15]. The phase shift due to the thermo-optically induced refractive index change is:

$$\Delta\phi = \frac{2\pi}{\lambda}(\partial n/\partial T)L\Delta T \quad (1)$$

where L is the length of the polymeric waveguide and ΔT is the temperature change. Therefore, by properly designing the heater length, the thermo-optically generated refractive index change can lead to a π phase shift for phase encoding. The phase coding scheme works for short (ps) optical pulses as well. This is because short optical pulses passing through a polymeric waveguide will experience the same refractive index change and therefore get the same phase shift through Equation (1). Note that the BPSK coding scheme is fixed for a specific channel. Each symbol of a specific channel is coded and decoded using the same code sequence of the channel.

Figure 2. Schematic structure of the thermo-optic (TO) phase encoder. It consists of a polymeric waveguide with a top electrode. The top electrode and the polymeric waveguide are separated by a cladding layer. Local heating in the polymeric waveguide can be achieved by applying current through the top electrode. The local current heater increase the temperature of the polymeric waveguide and lead to refractive index change through the TO effect of the polymeric waveguide. The refractive index change will result in phase shift of the optical signals in the waveguide.

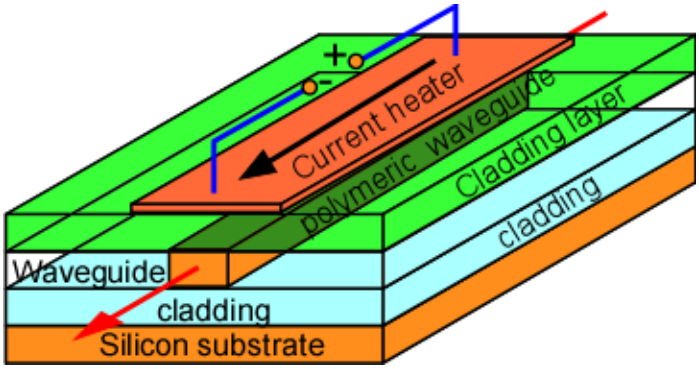

The polymeric waveguides in optical CDMA coding and decoding systems are standard single mode waveguides on silicon substrates. Detailed material compositions, fabrication procedures, and polymic waveguides' transmission properties have been reported elsewhere [16,17]. The TO effect in polymeric waveguides has been extensively studied [16,17]. The heating effect and the thermal-induced refractive index change are localized in a polymeric waveguide [16,17]. The thermal interference among different optical waveguides can be ignored [18]. The heating uses DC current. There is no EM interference between the channels. The waveguide, 1xN splitter and the combiner have the same waveguide dimension and refractive indices. The refractive indices are matched. The thermally induced refractive index change is small (~10^{-3}–10^{-4}). The small thermally induced refractive index change will generate reflection and loss fluctuation in an order of 0.1%.

As shown in Figure 1, in the encoder, each bit of the data (symbol) signals is encoded by 10 time-resolved pulse code generates BPSK signals called a code sequence. The code sequences can be written as:

$$X_k(t) = \sum_{m=0}^{M-1} b_m^k u(t - mT_c) \tag{2}$$

where, b_m^k is the BPSK codes for channel k, T_c is the chip pulse width, $u(t)$ is the pulse profile, and M is the length of the code. Ideally, the code sequences for individual channels should be orthogonal, *i.e.*,

$$R(\tau) = X_i(t) \otimes X_k(t) = \sum_{m=0}^{M-1}\sum_{n=0}^{M-1} b_n^i b_m^k u(t - nT_c - mT_c)u(nT_c + mT_c + \tau) = \delta_{i,k}\delta(\tau), \quad (3)$$

where, $R(\tau)$ is the channel correlation function. However, due to the short code length, the cross correlation function between the channels is non-zero. This is the cross correlation noise. The encoded signal $f_i(t)$ for each channel is given by the convolution of the data signal $s(t)$ and the code $X(t)$:

$$f_i(t) = s_i(t) \otimes X_i(t) = \sum_{n=0}^{K-1}\sum_{m=0}^{M-1} b_m^i u(t - mT_c - nT_s)s_i(mT_c + nT_s), \quad (4)$$

where, K is the length of the symbols. Defining N as the total number of channels in the Optical CDMA system, and T_s as the time duration for one signal bit, the total transmitted signal, $f(t)$, can be expressed as the summation of the encoded signal of each individual channel, *i.e.*,

$$f(t) = \sum_{i=1}^{N} f_i(t), \quad (5)$$

The received signal, $r(t)$, contains both the transmitted signal $f(t)$, and the additive noise $n(t)$ that is accumulated during transmission, *i.e.*,

$$r(t) = f(t) + n(t), \quad (6)$$

Figure 3 shows the schematic structure of the optical CDMA decoder for one channel. It consists of optical-time lines, optical combiners, and TO phase-decoders. The TO phase decoders are the same as in the optical CDMA encoder of the same channel. The optical CDMA decoders for other channels have the same structure with their own codes for the TO phase-decoders. The code for is fixed each for channel. The TO heater is always on. Therefore, the optical CDMA system is broadband. It can handle very short optical pulses in picosecond (ps) region.

In the receiver, the received signal, $r(t)$, is decoded by taking correlation with a specific code sequence (decoding sequence) of an individual channel. The decoding sequence is the same as the coding sequence of the same channel. The decoding sequences can be written as:

$$Y_k(t) = \sum_{m=0}^{M-1} d_m^k u(t - mT_c) \quad (7)$$

where, d_m^k is also the BPSK codes, k represents the channel number. The decoding sequences for individual channels are also orthogonal. The decoded signal for each individual channel, $g_i(t)$, is given by the convolution of the received signal with the code sequence:

$$\begin{aligned} g_i(t) = r(t) \otimes Y_k(t) &= \sum_{i}^{N} [f_i(t) + n(t)] \otimes Y_k(t), \\ &= \sum_{i}^{N} [s_i(t)X_i(t) \otimes Y_k(t) + n(t) \otimes Y_k(t)], \\ &= s_i(t) + \sum_{i}^{N} n(t) \otimes Y_k(t) \end{aligned} \quad (8)$$

The decoded data streams can be finally obtained. The last term represents the noise term. The second term represents the cross correlation noise.

Figure 3. Schematic structure of the optical CDMA decoder for one channel. It consists of optical-time lines, optical combiners, and TO phase-decoders. The TO phase decoders are the same as in the optical CDMA encoder of the same channel. The optical CDMA decoders for other channels have the same structure with their own codes for the TO phase-decoders.

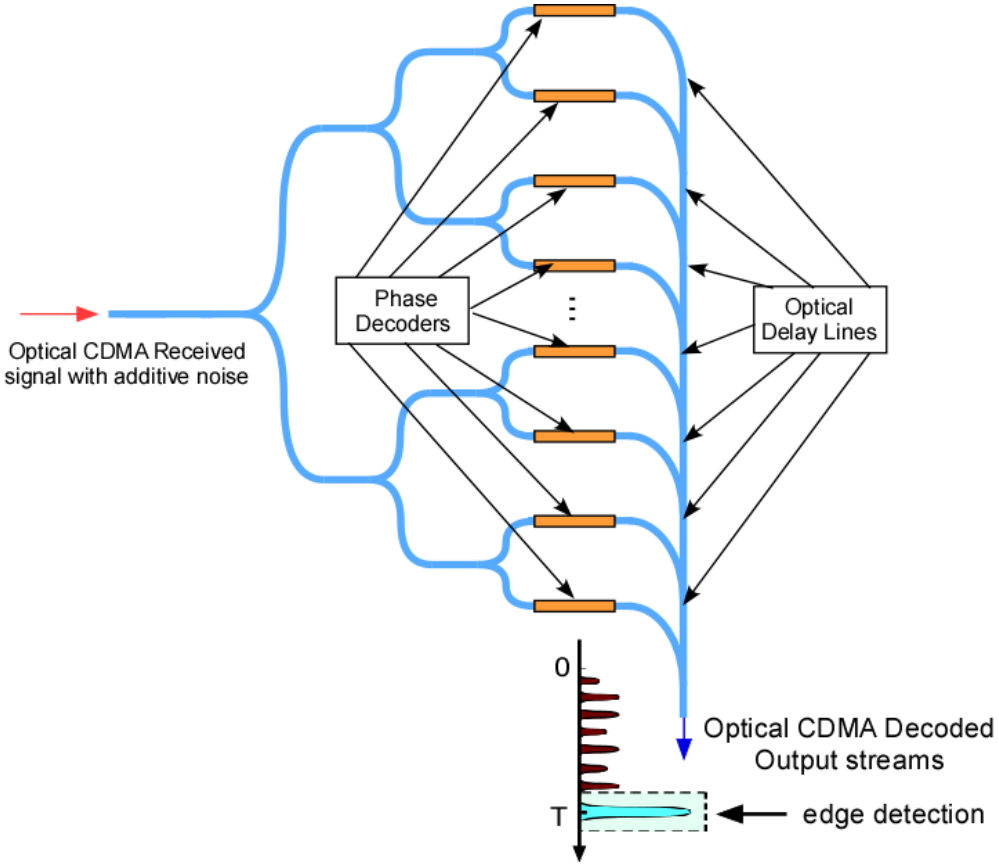

3. Results and Discussion

Numerical simulation is performed by using Equations (1–8) for two-channel 10-chip optical CDMA data streams. The data stream of each of the channels is encoded by its polymeric waveguide encoder with its own phase-coding (Equation (2)). Figure 4(a) shows the original data stream 1 0 1 1 1 0 1 0 of channel #1. The signal bits are in non-return-to-zero (NRZ) format. Each bit of the signal is 50 ps. Figure 4(b) shows the phase-coded data stream of channel #1 by using its phase code [0 π 0 0 0 π π 0 π 0]. Figure 5(a) shows the original data stream 1 1 0 0 1 1 0 1 of channel #2. Figure 5(b) shows the phase-coded data stream of channel #2 by using its phase code [0 π 0 0 π 0 0 0 0 π].

The received signals are shown in Figure 6. It contains the both phase-encoded channel #1 and channel #2 signals plus the additive noise accumulated in the transmission. Since Gaussian white noise is the most commonly used additive white noise source in communication system simulation, we use Gaussian white noise as the additive noise in the simulation. The probability density function (pdf) of Gaussian noise is equal to that of normal distribution. Since the typical decision level in a receiver is half-way between 1 and 0, which is 0.5, we choose the standard deviation 0.5 to be the same as the decision level.

Figure 4. (**a**) original data symbol 1 0 1 1 1 0 1 0 of channel #1. The signal bits are in non-return-to-zero (NRZ) format. Each bit of the signal is 50 ps; (**b**) phase-coded (BPSK) data stream of channel #1 using its phase code [0 π 0 0 0 π π 0 π 0].

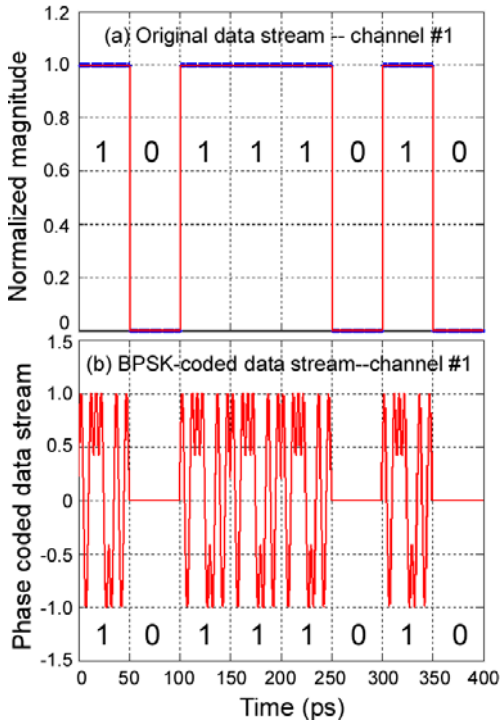

Figure 5. (**a**) original data stream 1 1 0 0 1 1 0 1 of channel #2; (**b**) phase-coded (BPSK) data stream of channel #2 using its phase code [0 π 0 0 π 0 0 0 0 π].

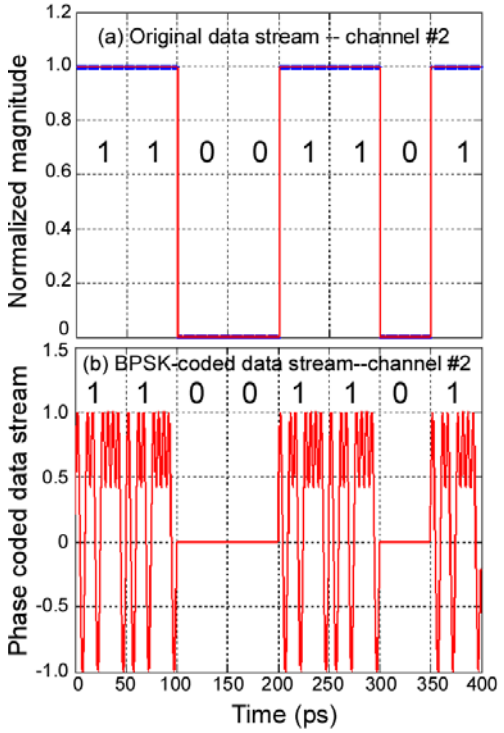

Figure 6. Received signals. It contains the both phase-encoded channel #1 and channel #2 signals plus the additive noise accumulated in the transmission. White noise with normal distribution is used as the additive noise in the simulation. The average value and the standard deviation of the normal noise are 0 and 0.5, respectively. The received signal is corrupted with interference from the other channel and the additive noise.

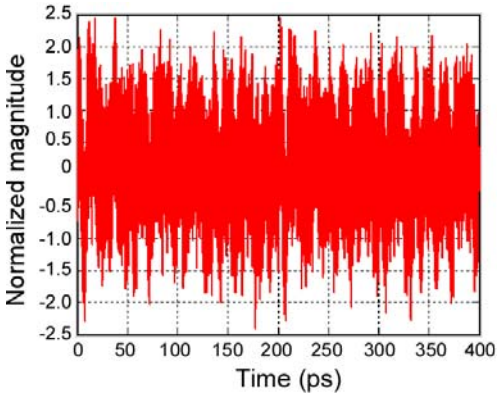

As shown in Figure 6, the received signal is corrupted with interference from the other channel and the additive noise. Figure 7(b) shows the decoded signal using the optical CDMA decoder with the code of [0 π 0 0 0 π π 0 π 0] for channel #1. For a better illustration, the original channel #1 symbols (Figure 4(a)) are reshown in Figure 7(a). The detection is edge-detection at the end of each 50-ps signal bit. The edge detection is achieved by a time-gated photodetector, *i.e.*, the detector is on for signal collection only at the end of each 50-ps signal bit. The signals of any other time are not collected. If there is a signal at the end of multiple of 50-ps, it is 1, otherwise it is 0. Using the edge detection, the original channel #1 data stream 1 0 1 1 1 0 1 0 can be recovered. Similarly, Figure 8(b) shows the decoded signal using the code of [0 π 0 0 π 0 0 0 π] for channel #2. The original channel #2 symbols (Figure 5(a)) are reshown in Figure 8(a). The original channel #2 data stream 1 1 0 0 1 1 0 1 can be recovered using the edge-detection as well.

The noise floor of the decoded signal is related the cross correlation of the code sequence. The signal-to-noise ratio (SNR) is given by [5]:

$$SNR = 4\left[\frac{M^3}{(N-1)(M^2+M-1)}\right], \tag{8}$$

where, M is the code length of the BPSK code for each channel, and N is the number of simultaneous users. Figure 5 shows the calculated SNR (dB) for different BPSK code lengths and different number of simultaneous users. As shown in Figure 9, the increase of the number of simultaneous users will significantly degrade the SNR of the received signal. This indicates that the cross correlation with other channels are the dominant source of noise for the received signal. A higher SNR can be obtained by increasing the BPSK code length (chip number) and decreasing the cross correlation with other channels.

Figure 7. (**a**) the original #1 symbols (reshown from Figure 4(a) for better illustration); (**b**) decoded signal using the optical CDMA decoder with the code of [0 π 0 0 0 π π 0 π 0] for channel #1. Using edge-detection at the end of each 50-ps signal bit, the original channel #1 data stream 1 0 1 1 1 0 1 0 can be recovered.

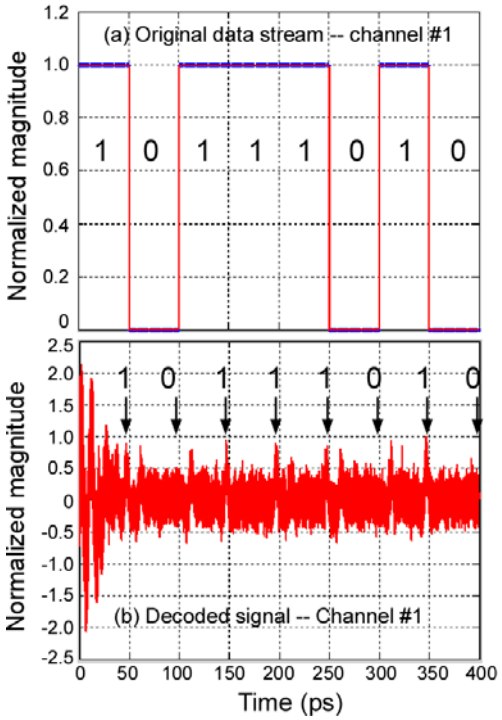

Figure 8. (**a**) the original #2 symbols (reshown from Figure 5(a) for better illustration); (**b**) decoded signal using with the code of [0 π 0 0 π 0 0 0 0 π] for channel #2. The original channel #2 data stream 1 1 0 0 1 1 0 1 can be recovered using the edge-detection.

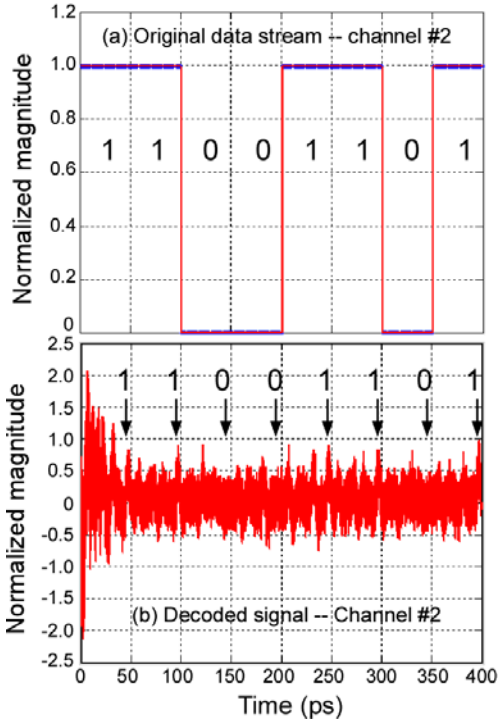

Figure 9. Calculated signal to noise ratio (SNR) for different binary phase-shift keying (BPSK) code length.

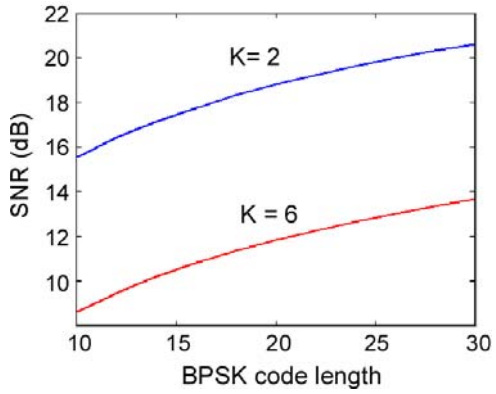

4. Conclusions

We proposed a low cost polymeric waveguide based optical CDMA encoder and decoder modules for FTTH applications. The performance of the optical CDMA encoder and decoder modules is simulated using 10-chip BPSK coding schemes. The optical CDMA encoder and decoder modules can effectively transmit and recover optical CDMA data streams. The simulation shows the polymeric optical CDMA encoder and decoder modules are promising for all-optical CDMA applications.

Reference

1. Viterbi, A.J. *CDMA Principles of Spread Spectrum Communication*; Addison-Wesley: Boston, MA, USA, 1995.
2. Liberti, J.C., Jr.; Rappaport, T.S. *Smart Antennas for Wireless Communications: IS-95 and Third Generation CDMA Applications*; Prentice Hall: Upper Saddle River, NJ, USA, 1999.
3. Salehi, J.A.; Brackett, C.A. Code division multiple-access techniques in optical fiber networks I. Fundamental principles. *IEEE Trans. Commun.* **1989**, *37*, 824-833.
4. Prucnal, P.R.; Santoro, M.A.; Fan, T.R. Spread spectrum fiber-optic local area network using optical processing. *J. Lightwave Technol*. **1986**, *LT-4*, 547-554.
5. Marhic, M.E. Coherent optical CDMA networks. *J. Lightwave Technol*. **1993**, *11*, 854-863.
6. Wada, N.; Kitayama, K. A 10 Gb/s optical code division multiplexing using 8-chip optical bipolar code and coherent detection. *J. Lightwave Technol.* **1999**, *17*, 1758-1765.
7. Tsuda, H.; Takenouchi, H.; Ishii, T.; Okamoto, K.; Goh, T.; Sato, K.; Hirano, A.; Kurokawa, T.; Amano, C. Spectral encoding and decoding of 10 Gbit/s femtosecond pulses using high resolution arrayed-waveguide grating. *Electron. Lett.* **1999**, *35*, 1186-1187.
8. Salehi, J.A.; Weiner, A.M.; Heritage, J.P. Coherent ultrashort light pulse CDMA communication systems. *J. Lightwave Technol.* **1990**, *8*, 478-491.
9. Seo, B.J.; Kim, S.; Fetterman, H.; Steier, W.; Jin, D.; Dinu, R. Design of ring resonators using electro-optic polymerwaveguides. *J. Phys. Chem. C* **2008**, *112*, 7953-7958.
10. Steiera, W.H.; Chen, A.; Leea, S.-S.; Garnera, S.; Zhang, H.; Chuyanova, V.; Dalton, L.R.; Wang, F.; Ren, A.S.; Zhang, C.; *et al*. Polymer electro-optic devices for integrated optics. *Chem. Phys*. **1999**, *245*, 487-506.

11. Chen, D.; Fetterman, H.R.; Chen, A.; Steier, W.H.; Dalton, L.R.; Wang, W.; Shi, Y. Demonstration of 110 GHz electro-optic polymer modulators. *Appl. Phys. Lett.* **1997**, *70*, 3335-3337.
12. Wang, W.; Chen, D.; Fetterman, H.R.; Shi, Y.; Steier, W.H.; Dalton, L.R.; Chow, P.-M.D. Optical heterodyne detection of 60 GHz electro-optic modulation from polymer waveguide modulators. *Appl. Phys. Lett.* **1995**, *67*, 1806-1809.
13. An, D.; Shi, Z.; Sun, L.; Taboada, J.M.; Zhou, Q.; Lu, X.; Chen, R.Y.; Tang, S.; Zhang, H.; Steier, W.H.; *et al*. Polymeric electro-optic modulator based on 1 × 2 Y-fed directional coupler. *Appl. Phys. Lett.* **2000**, *76*, 1972-1975.
14. Cheng, Y.J.; Luo, J.; Hau, S.; Bale, D.H.; Kim, T.D.; Shi, Z.; Lao, D.B.; Tucker, N.M.; Tian, Y.; Reid, P.J.; Dalton, L.R.; Jen, A.K.-Y. Large electro-optic activity and enhanced thermal stability from Diarylaminophenyl-containing High-b nonlinear optical chromophores. *Chem. Mater.* **2007**, *19*, 1154-1163.
15. Peyghambarian, N.; Dalton, L.; Jen, A.K.-Y.; Kippelen, B.; Marder, S.R.; Norwood, R.; Perry, J.W. Recent advances in organic nonlinear optics. *Laser Focus World* **2006**, *43*, 85-92.
16. Wang, X.; Howley, B.; Chen, M.Y.; Zhou, Q.; Chen, R.; Basile, P. Polymer based thermo-optic switch for optical true time delay. *Proc. SPIE* **2005**, *5728*, 60-67.
17. Yang, J.; Zhou, Q.; Chen, R.T. Polyimide-waveguide-based thermal optical switch using total-internal-reflection effect. *Appl. Phys. Lett.* **2002**, *81*, 2947-2949.
18. Jang, C.-H.; Chen, R.T. Polymer-based 1 × 6 thermooptic switch incorporating an elliptic TIR waveguide mirror. *J. Lightwave Technol.* **2003**, *21*, 1053-1058.